PAPER

An Explanation of Signal Changes in DW-fMRI: Monte Carlo Simulation Study of Restricted Diffusion of Water Molecules Using 3D and Two-Compartment Cortical Cell Models

Shizue NAGAHARA[†,††a)], ***Student Member***, **Takenori OIDA**[†], ***and*** **Tetsuo KOBAYASHI**[†], ***Members***

SUMMARY Diffusion-weighted (DW)-functional magnetic resonance imaging (fMRI) is a recently reported technique for measuring neural activities by using diffusion-weighted imaging (DWI). DW-fMRI is based on the property that cortical cells swell when the brain is activated. This approach can be used to observe changes in water diffusion around cortical cells. The spatial and temporal resolutions of DW-fMRI are superior to those of blood-oxygenation-level-dependent (BOLD)-fMRI. To investigate how the DWI signal intensities change in DW-fMRI measurement, we carried out Monte Carlo simulations to evaluate the intensities before and after cell swelling. In the simulations, we modeled cortical cells as two compartments by considering differences between the intracellular and the extracellular regions. Simulation results suggested that DWI signal intensities increase after cell swelling because of an increase in the intracellular volume ratio. The simulation model with two compartments, which respectively represent the intracellular and the extracellular regions, shows that the differences in the DWI signal intensities depend on the ratio of the intracellular and the extracellular volumes. We also investigated the MPG parameters, b-value, and separation time dependences on the percent signal changes in DW-fMRI and obtained useful results for DW-fMRI measurements.

key words: *functional magnetic resonance imaging, diffusion-weighted imaging, restricted diffusion, Monte Carlo method*

1. Introduction

Various tools such as electroencephalograms, magnetoencephalograms, near-infrared spectroscopy, and functional magnetic resonance imaging (fMRI) are available for measuring the human brain activity noninvasively. Among these tools, fMRI is widely used because of its ease of use and relatively high spatial resolution. However, the fMRI method used currently is based on the blood-oxygenation-level-dependent (BOLD) effect, and it is used to observe the hemodynamic responses following neuronal activations, thus limiting the spatial and temporal resolutions.

Recently, an increased number of studies have used DW-fMRI [1]–[5]. This approach is based on the property that cortical cells (neurons and glial cells) in the brain swell when the brain is activated [1], [6]. Cell swelling causes changes in the apparent diffusion coefficients of water molecules before and after brain activation [1], [2]. This results in changes in the diffusion-weighted imaging (DWI) signal intensities. However, there is much debate on the exact mechanism of this approach [7]–[9]. Moreover, DWI signal intensities depend on complicated imaging parameters, and several issues regarding DW-fMRI remain to be clarified.

In our previous study, we showed the importance of choosing certain DW-fMRI parameters and observed the influences of these parameters on the DWI signal intensities by using Monte Carlo simulations [10]. In the study, we employed a simple 2D circle simulation model with only one component to determine the influence of the size of the restricted structures and to simplify the required calculations. We assumed the presence of water molecules around cortical cells while ignoring the differences between the intracellular and the extracellular regions. Thus, we could not simulate the changes in water diffusion in the intracellular and the extracellular regions simultaneously.

In the present study, we improved our simulation model to a 3D cube with two compartments, corresponding to the intracellular and the extracellular regions, and we investigated the DWI signal intensities and the differences between them before and after cell swelling. By using this simulation model with two compartments, we can discriminate the intracellular and the extracellular regions and observe not only the changes in DWI signal intensities in each region individually but also the changes in the total DWI signal intensities. Moreover, we can observe how water molecules in the two regions affect the DWI signal intensities simultaneously. Our new models should enable the implementation of a more detailed simulation.

In the DW-fMRI method, we observed that the DWI signal intensities changed because of changes in the apparent diffusion coefficients of water molecules. To investigate how and why the DWI signal intensities change, i.e., how and why the apparent diffusion coefficients change after cell swelling, we estimated the DWI signal intensities by using Monte Carlo simulations.

2. Background

DWI is an imaging technique that incorporates MRI to visualize the self-diffusion of water. DWI can show complex and minute structures in cells by observing the diffusion of water molecules within various structures [11], [12]. DWI

Manuscript received October 2, 2012.
Manuscript revised December 27, 2012.

[†]The authors are with the Graduate School of Engineering, Kyoto University, Kyoto-shi, 615–8510 Japan.
[††]The author is a research fellow of the Japan Society for the Promotion of Science.
a) E-mail: nagahara@bfe.kuee.kyoto-u.ac.jp

DOI: 10.1587/transinf.E96.D.1387

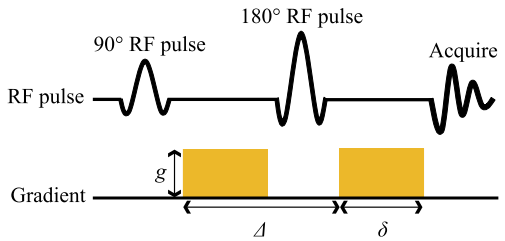

Fig. 1 Stejskal-Tanner's pulse sequence that is generally used for DWI. A pair of gradients with the same amplitude and period is applied on both sides of the 180° refocus pulse.

can be used to obtain images by applying a pair of gradients, called as motion probing gradients (MPGs), on both sides of a 180° refocus pulse of a spin-echo pulse sequence. An example of a DWI pulse sequence is shown in Fig. 1.

The DWI signal intensities are calculated by using the following equation:

$$S = S_0 \exp(-b \cdot D), \tag{1}$$

where S_0 is the signal intensity without MPG, and b is the b-value expressed as follows:

$$b = \gamma^2 g^2 \delta^2 \left(\Delta - \frac{\delta}{3}\right), \tag{2}$$

where γ is the gyromagnetic ratio of protons, which is $2\pi \times 42.58 \times 10^6$ rad/s·T, and g, δ, and Δ are the amplitude, duration time, and separation time of the MPG, respectively, as shown in Fig. 1. D is the diffusion coefficient. In the case of restricted diffusion, for example, water diffusion in living bodies, we have to use an apparent diffusion coefficient instead of the diffusion coefficient because water diffusion is affected by obstacles such as cell membranes. In this study, we use D as the apparent diffusion coefficient to consider restricted diffusion.

In the case of restricted diffusion, Δ offers water molecules a long time to diffuse during the DWI measurement. In addition, the number of collisions of water molecules with obstacles increases for large Δ. Thus, D appears smaller than the true diffusion coefficient of water molecules.

Moreover, when cell swelling occurs, the apparent diffusion coefficient of water molecules changes in the intracellular and the extracellular regions. This is because cell swelling expands the intracellular region and shrinks the extracellular region and the distance which water molecules can move for changes in both regions. Hence, the influence of Δ on the diffusion of water molecules changes in the expanded intracellular region and the shrunk extracellular region. For these reasons, D is affected by both Δ and changes in the size of restricted regions derived from cell swelling, and DWI signal intensities are also affected by these two factors as is obvious in Eq. (1). Therefore, we should carefully consider the effects of Δ as well as the b-value and also the size of restricted regions in DW-fMRI measurement.

3. Methods

3.1 Simulation Model

Cortical cells in the brain primarily consist of neurons and glial cells that swell upon brain activation [6]. In this simulation, we modeled the water diffusion around cells whose diameters were approximately 5–100 μm [13], and we employed a 3D cubic simulation model (Fig. 2) with two compartments. The cells are modeled as cubes; the inner region of the cube with solid lines indicates the intracellular region, and the region outside these lines indicates the extracellular region.

We assumed that water molecules diffused according to a normal distribution and were reflected at the solid lines, which are the boundaries between the intracellular and the extracellular regions, as shown in Fig. 2. Water molecules in the extracellular region diffused through the dotted lines, which are the boundaries for the units of calculation. Water molecules are reflected at the surface of the outer cubes. The effects of reflection at the surface of the outer cubes should be considered because water diffusion in the extracellular region is restricted. Therefore, we set as many cubic units as possible in the outer cube and decreased the ratio of volumes in which water molecules are reflected at the surface of the outer cube.

In this simulation, we calculated the changes in positions and the phase of the magnetization precession of protons in water molecules diffusing near restricted structures.

3.2 Algorithm

Simulations were conducted using Microsoft Visual C++.

1. We used an outer cube with a length of $2L$ on each side, which included X cubes with a length of $2r$ on each side, in the 3D space as a simulation model. This cube was divided into X sub-sections with lengths of $2l$ on each side. These sub-sections were referred to as units. X cubes in the intracellular regions were regularly spaced in three directions and separated by the extracellular region at an interval of $2l - 2r$.
2. We arranged Z water molecules whose default positions were distributed uniformly in the outer cube.
3. We set Δt as a time step and renewed the position of each water molecule according to the Einstein-Smoluchowski equation. We renewed the positions of each water molecule according to a normal distribution with mean 0 and variance $2D\Delta t$ in each direction as follows:

$$\begin{aligned} \mathbf{p}_k(t + \Delta t) &= \mathbf{p}_k(t) + N[\mathbf{a}, \mathbf{C}] \\ k &= 1, 2, 3, \cdots, Z \\ \mathbf{a} &= (0 \quad 0 \quad 0) \\ \mathbf{C} &= \begin{pmatrix} 2D\Delta t & 0 & 0 \\ 0 & 2D\Delta t & 0 \\ 0 & 0 & 2D\Delta t \end{pmatrix} \end{aligned} \tag{3}$$

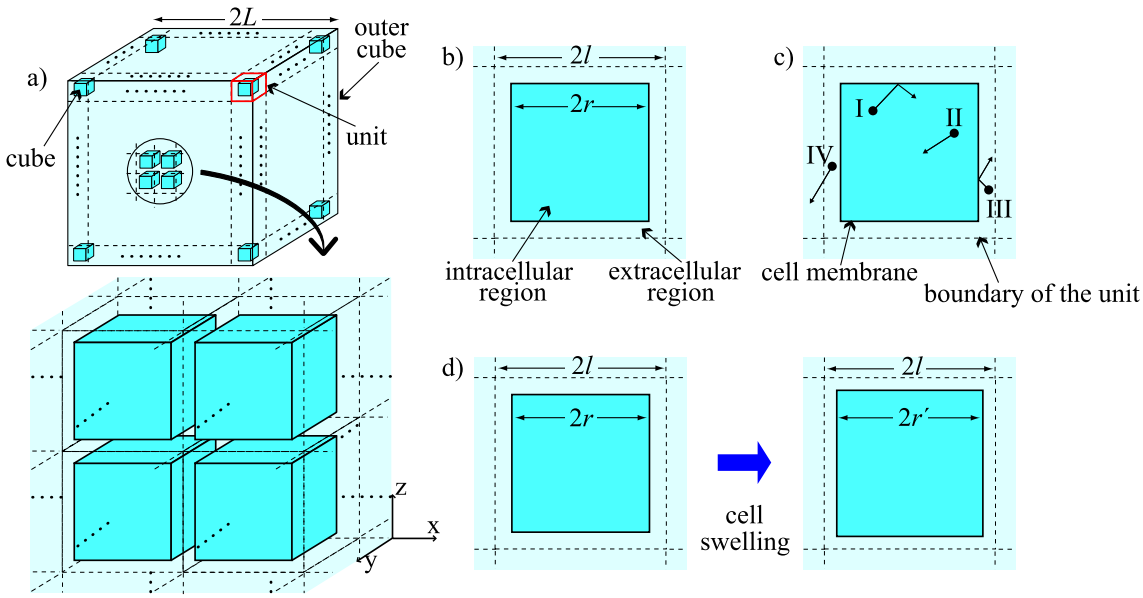

Fig. 2 3D cubic simulation model with two compartments. (a) Cubic cells are arranged regularly in the x, y, and z directions. (b) Dark- and light-color regions represent the intracellular and the extracellular regions, respectively. (c) Solid lines indicate the boundaries of the intracellular and the extracellular regions and mean cell membranes. Dotted lines indicate the boundaries of the units used for calculation. In the intracellular region, water molecules that reach the solid lines are reflected (I). Water molecules that do not reach the solid lines diffuse within the intracellular region (II). In the extracellular region, water molecules that reach the solid lines are reflected (III). Water molecules that reach the dotted lines diffuse through the dotted lines (IV). (d) With respect to cell swelling, the size of the cubic cells increased from $2r$ to $2r'$, whereas that of the cubic units did not change.

where $\mathbf{p}_k(t+\Delta t)$ is the position of each water molecule, and $N[\mathbf{m}, \sigma^2]$ is a 3D random number following a normal distribution with mean $\mathbf{m}$ and variance σ^2. When a water molecule reached the intracellular and the extracellular boundaries or the surface of the outer cube, we renewed its position to reflect that it was at the boundary or surface.

4. We renewed the phases of transverse magnetization in each water molecule, while MPG was applied according to the Stejskal-Tanner plus sequence shown in Fig. 1. Thus, phase changes (θ) at every coordinate axis were calculated as follows:

$$\theta_{k,i}(t) = \gamma g_i \int_t^{t+\Delta t} p_{k,i}(\tau) d\tau \qquad (4)$$
$$k = 1, 2, 3, \cdots, Z$$
$$i = x, y, z$$

where g_x, g_y, and g_z are the amplitudes of MPG along the x-, y-, and z-axis, respectively. In addition, all phases were inverted when the 180° RF pulse was applied. The phase of each water molecule obtained at $t = TE$ was calculated as follows:

$$\theta_{k,i} = -\sum_{j=0}^{n} \theta_{k,i}(j\Delta t) + \sum_{j=0}^{n} \theta_{k,i}(\Delta + j\Delta t) \qquad (5)$$
$$k = 1, 2, 3, \cdots, Z$$
$$i = x, y, z$$
$$n = \frac{\delta}{\Delta t}$$

where the first MPG was applied at $t = 0$. TE is an echo time.

5. We calculated the normalized signal intensity E of DWI from the phases of transverse magnetization as follows:

$$E = \frac{S}{S_0}$$
$$= \frac{1}{Z}\sqrt{\left(\sum_{k=1}^{Z} \cos\theta_k\right)^2 + \left(\sum_{k=1}^{Z} \sin\theta_k\right)^2} \qquad (6)$$
$$\theta_k = \theta_{k,x} + \theta_{k,y} + \theta_{k,z}$$

where S is the signal intensity with MPG and S_0, that without MPG.

6. We obtained the final normalized signal intensities by repeating the same procedure M times and calculating the average of all normalized signal intensities.

3.3 Simulations of Restricted Diffusion

First, we investigated how the DWI signal intensities change in the intracellular and the extracellular regions after cell swelling. We calculated the normalized signal intensities in the intracellular and the extracellular regions as well as the total DWI signal intensities when the size of cubic cells changes in our model. We set the b-value to 1000 s/mm^2 while changing the r range. These parameters are shown in Table 1.

Table 1 MPG parameters for simulations to determine r dependences in the intracellular and the extracellular regions.

b [s/mm^2]	$2r$ [μm]	g [mT/m]	δ [ms]	Δ [ms]
1000	10.0 ≀ 11.0	$25\sqrt{3}$	13.56	45.05

Table 2 MPG parameters for simulations to determine Δ dependence.

b [s/mm^2]	$2r$ [/mm]	$2r'$ [/mm]	g [mT/m]	δ [ms]	Δ [ms]
1000	10.0	10.1 ≀ 11.0	$25\sqrt{3}$	10.85 ≀ 22.24	66.94 ≀ 22.48
2000	10.0	10.1 ≀ 11.0	$25\sqrt{3}$	10.85 ≀ 27.66	130.27 ≀ 28.70
3000	10.0	10.1 ≀ 11.0	$25\sqrt{3}$	10.85 ≀ 32.00	193.59 ≀ 32.50

Table 3 MPG parameters for simulations to observe b-value dependence.

b [s/mm^2]	$2r$ [/mm]	$2r'$ [/mm]	g [mT/m]	δ [ms]	Δ [ms]
500 ≀ 2400	10.0	10.1 ≀ 11.0	$25\sqrt{3}$	11.97 ≀ 29.87	30
500 ≀ 3000	10.0	10.1 ≀ 11.0	$25\sqrt{3}$	9.44 ≀ 24.65	45
500 ≀ 3000	10.0	10.1 ≀ 11.0	$25\sqrt{3}$	8.07 ≀ 20.51	60

Table 4 Values of parameters Z, Δt, D_{int}, D_{ext}, and M were used in all simulations.

Z	Δt [μs]	D_{int} [mm^2/s]	D_{ext} [mm^2/s]	M
10^6	100	1.0×10^{-3}	3.0×10^{-3}	10

Next, we observed the percent signal changes ΔE by assuming that the size of the cubic cells increases from 10.0 μm to 10.1–11.0 μm. The simulation offered Δ and the b-value dependences of ΔE to show how large ΔE becomes after cell swelling under our assumption. Moreover, the simulation was also implemented to show how ΔE depends on these parameters. The parameters of these simulations are shown in Tables 2 and 3.

In every simulation, we set $2r$ to 10 μm to consider the size of the cell and $2l$ to 11.262 μm to set the volume ratio of the intracellular and the extracellular regions to 70% [14], [15]. Moreover, we assumed that a cell with a length of 10 μm on each side swelled by 1–10% in length, while $2l$ is fixed to 11.262 μm. $2L$ was fixed to 112.62 μm, resulting in $X = 10$. In the simulations, water molecules were reflected at the surface of the outer cube. We also set D_{int} to 1.0×10^{-3} mm^2/s and D_{ext} to 3.0×10^{-3} mm^2/s [14], [15]. The remaining parameters were $Z = 10^6$, $\Delta t = 100\,\mu$s, and $M = 10$. These parameters were fixed for every simulation, as shown in Table 4. To investigate the influence of the diffusion of water molecules on DWI signals, we focused on the normalized signal intensities while ignoring the T_2 decay.

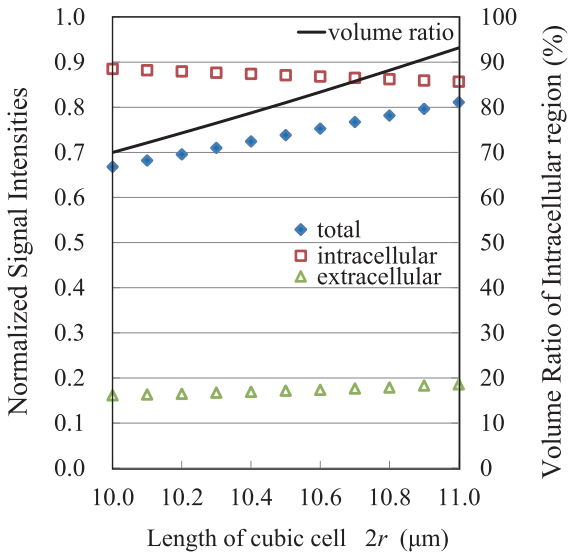

Fig. 3 Normalized signal intensities E as a function of $2r$ for b-values of 1000 s/mm^2 and Δ of 45.05 ms, when $g = 25\sqrt{3}$ mT/m; total signal intensities (♦), intracellular ones (□), extracellular ones (△), and intracellular volume ratio (–).

4. Results

Simulation results of the intracellular and the extracellular regions are shown in Fig. 3 for a b-value of 1000 s/mm^2. These results show the normalized signal intensities with changes in the length of the cubic cell. Squares and triangles indicate the normalized signal intensities in the intracellular and the extracellular regions, respectively. These results show that the DWI signal intensities decrease with an increase of $2r$ in the intracellular region, whereas the intensities increase with an increase of $2r$ in the extracellular region. These changes in the DWI signal intensities result from changes in the apparent diffusion coefficients. In the intracellular region, water molecules can move for a longer distance when $2r$ increases, and therefore, the apparent diffusion coefficient of this region seems to increase with larger $2r$. In contrast, in the extracellular region, the restriction for the movement of water molecules becomes stronger when $2r$ increases, and therefore, the apparent diffusion coefficient of this region seem to decrease with larger $2r$. Figure 3 also shows that the DWI signal intensity is much larger in the intracellular region than in the extracellular region. The reason for these results is that the apparent diffusion coefficient in the intracellular region is much smaller than that in the extracellular region.

Moreover, diamonds and a solid line indicate the total normalized signal intensities and the intracellular volume ratio, respectively. Considering the volume ratio between the intracellular and the extracellular region, the intracellular volume is much larger than the extracellular one, and then, the contribution of the intracellular region to total DWI signal intensities is supposed to be dominant. Therefore, we can interpret that the total DWI signal intensities decrease

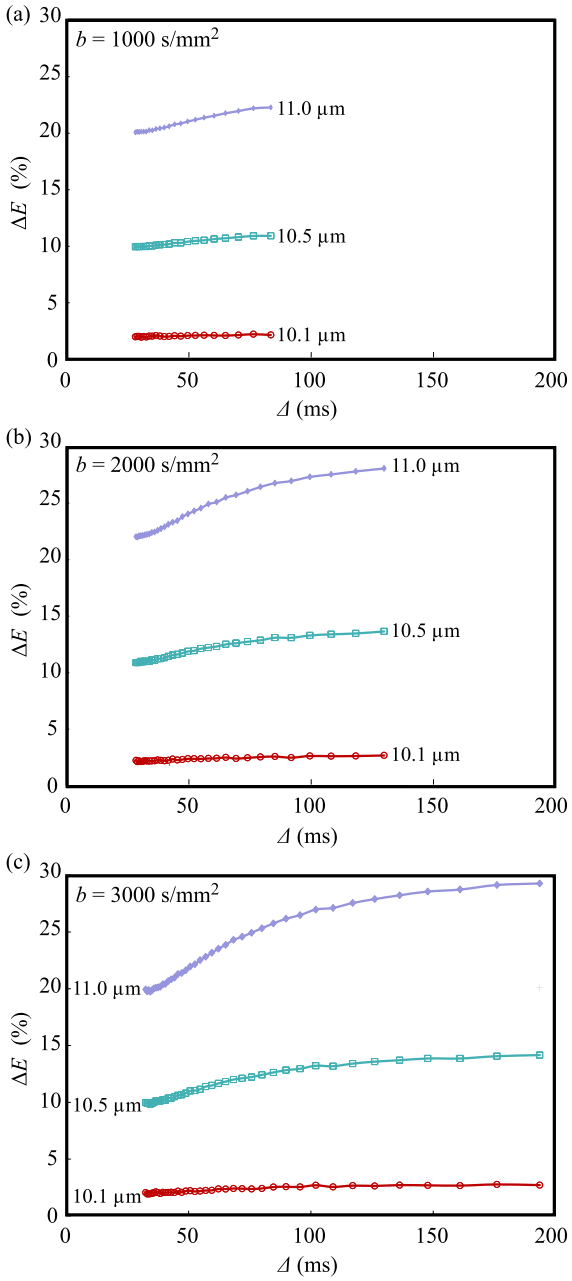

Fig. 4 Percent signal change ΔE as a function of Δ for b-values of 1000 s/mm^2 (a), 2000 s/mm^2 (b), and 3000 s/mm^2 (c), when $g = 25\sqrt{3}$ mT/m. $\Delta E = (E' - E)/E \times 100$, where E represents the normalized signal intensities observed before cell swelling and E' represents those observed after cell swelling.

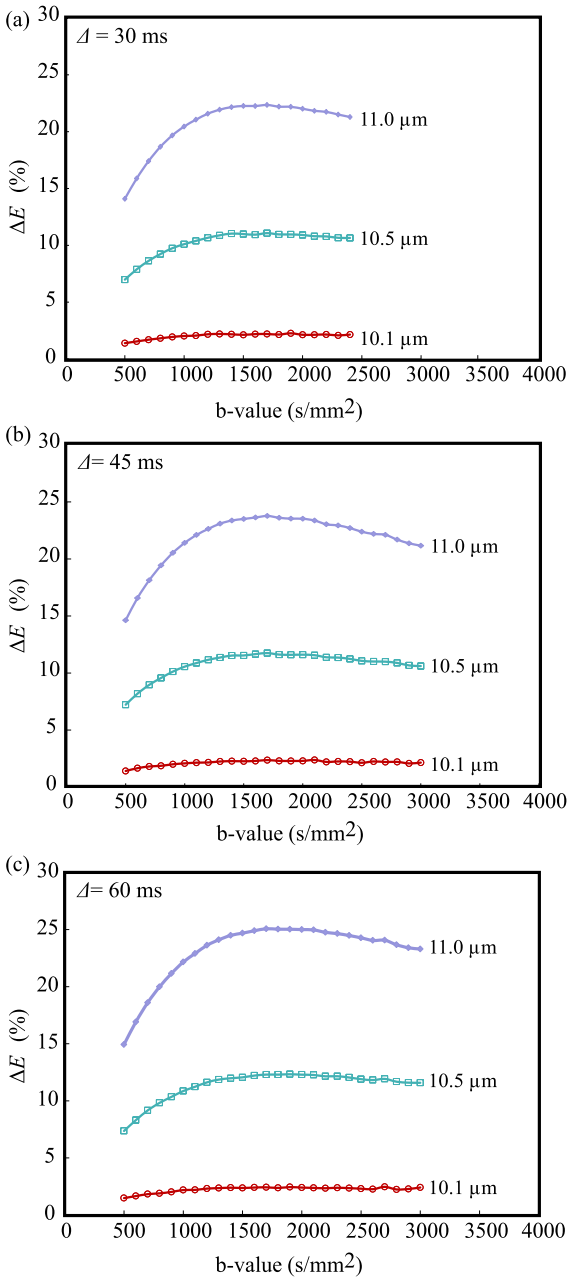

Fig. 5 Percent signal change ΔE as a function of b-value for Δ of 30 ms (a), 45 ms (b), and 60 ms (c) when $g = 25\sqrt{3}$ mT/m. $\Delta E = (E'-E)/E \times 100$, where E represents the normalized signal intensities observed before cell swelling and E' represents those observed after cell swelling.

after cell swelling because these intensities decrease in the intracellular region. The diamonds, however, suggest that the total normalized signal intensities increase with an increase in $2r$. This is because the intracellular volume ratio increases, and the ratio of water molecules in the intracellular region, which have larger DWI signal intensities, increases. According to these results, we can conclude that the increases in the intracellular volume ratio have a greater effect on the changes in the total DWI signal intensities than the DWI signal changes in each region.

Figure 4 shows the percent signal change ΔE as the length of the cubic cells is increased from 10.0 μm to 10.1–11.0 μm, assuming cell swelling. We set the b-value to 1000 s/mm^2 (a), 2000 s/mm^2 (b), and 3000 s/mm^2 (c) and changed Δ to investigate the Δ dependences of ΔE. ΔE increased with an increase in Δ for all b-value settings.

We also examined the b-value dependence of ΔE with the change in cell size. Figure 5 shows the results of using Δ values of 30 ms (a), 45 ms (b), and 60 ms (c) assuming that the cell size increases from 10 μm to 10.1–11.0 μm. As

in the case of the simulation results of the Δ dependence, ΔE increased after cell swelling. From the results of the b-value dependence, we obtained the largest ΔE for a b-value of 1500–2000 s/mm^2. Thus, we expect larger ΔE values using such b-values in DW-fMRI experiments.

5. Discussion

We simulated the diffusion of water molecules and investigated the changes in the DWI signal intensities after cell swelling. In the simulation, we assumed that water molecules do not pass through the cell membrane (except when cell swelling occurs) in order to observe how water diffusion affects the differences in the normalized signal intensities of DW-fMRI and to simplify the calculations. We also assumed that the density ratio of water molecules in the intracellular and the extracellular regions was constant during cell swelling.

We expanded our previous simulation model in the present study to consider the influence of the intracellular and the extracellular regions on the DWI signal intensities in DW-fMRI. As we showed in the result section, we obtained increased normalized signal intensities after cell swelling. This is because in the present simulation model with two compartments, we could observe the increase in the intracellular volume ratio. This implies that the increase in the number of water molecules in the intracellular regions, which have smaller apparent diffusion coefficients, results in larger DWI signal intensities after cell swelling. On the other hand, in our previous simulation model with one compartment, we could only observe a change in the apparent diffusion coefficients of water molecules because the size of the restricted region increases.

Our previous simulation model has only one compartment modeling intracellular region and we could calculate the movement of water molecules only in that compartment. In that model, we assumed that the intracellular regions expand due to cell swelling. Therefore, the apparent diffusion coefficient increases and the normalized signal intensity decreases, which can be seen in Fig. 3 as the decrease of the normalized signal intensities in the intracellular regions (□). We obtained the same results in our previous study [10].

In contrast, Fig. 3 shows that the total normalized signal intensity increases when the size of cell increases. This is because the signals in the extracellular regions and the intracellular volume ratio increase. This result might represent the advantage of the present model.

Previous studies by other groups [1]–[5] observed increased signals in DW-fMRI. For instance, a study showed decreased apparent diffusion coefficient, implying increased normalized signal intensity for about 1.57% with b-value of 1443–1461 mm^2/s and this result was consistent with our result that the normalized signal intensities increased for about 2.17% with b-value of 1400 mm^2/s, Δ of 30 ms, and r' of 10.1 μm [1]. In other studies, 1–2% increases of the raw signal intensities with the b-value of 1600–1800 mm^2/s were reported [2], [3], [5]. In our simulations, we obtained 2.15–2.18% increases in the normalized signal intensities with the b-value of 1600–1800 mm^2/s, Δ of 30 ms, and r' of 10.1 μm. Moreover, another study showed the normalized signal increases about 2–3% with b-value of 1800 mm^2/s, which is comparable with 2.15% signal increase with b-value of 1800 mm^2/s [4], Δ of 30 ms and r' of 10.1 μm in the present simulation results. These facts suggest that the present simulation model with two compartments is more reliable than our previous simulation model with one compartment.

Moreover, we obtained not only ΔE before and after cell swelling but also the Δ and b-value dependences on ΔE. The simulation results showed ΔE after cell swelling as a function of Δ with three b-values; a similar tendency was observed for all b-values. Δ has a significant role in the DWI measurement, and, of course, in DW-fMRI, when focusing on restricted diffusion. In the human brain, water molecules undergo restricted diffusion, and therefore, we should consider the effects of Δ in DW-fMRI. As shown in Fig. 4, we determined how Δ affects ΔE. However, it should be ensured that the separation time Δ is shorter than TE. If TE is too long, the normalized signal intensities decay to a great extent. The TE value in DWI is typically of the order of hundreds of milliseconds, although we use a stimulated echo sequence to avoid decay in signal intensities for long TE in DWI [16], [17]. Therefore, we should select Δ smaller than TE in practical use.

In addition to the Δ dependence, we also observed ΔE after cell swelling as a function of the b-value. Figure 5 shows that the b-value has an optimal value that emphasizes ΔE while Δ is fixed. A large b-value provides large δ with fixed Δ and g. In addition, large δ provides large θ because the large δ stacks the changes in θ, which can be seen in Eq. (4). However, we should consider that θ larger than π or smaller than $-\pi$ is equal to $(\theta - \pi)$ or $(\theta + \pi)$, respectively, in the DWI signal intensities. Therefore, if we use a large b-value, we can obtain many water molecules with θ larger than π or smaller than $-\pi$, and we cannot reflect the diffusion of water molecules to the DWI signal intensities exactly. Then, there might be an optimal range of b-values for DWI and DW-fMRI. This result implies that the b-value also plays a significant role when we observe ΔE in DW-fMRI. In this regard, in a previous study by another group [2], we found that a b-value consistent with our proposal (around 2000 s/mm^2) was used. As for Δ, TE was set to 87 ms, and therefore, we should select as small a value of Δ as possible in order to set TE to ∼90 ms considering experimental studies.

6. Conclusion

We investigated how and why DWI signal intensities change after cell swelling in DW-fMRI measurements. We used the Monte Carlo method to calculate the differences between the normalized signal intensities before and after cell swelling by simulating the diffusion of water molecules within restricted structures. In this simulation, we employed a 3D

simulation model with two compartments, respectively representing the intracellular and the extracellular regions, in order to distinguish the contributions of these two regions. Our simulation results using this model showed that the DWI signal intensities increase after cell swelling. These results could be interpreted because of the increasing ratio of the intracellular volume, which has a smaller diffusion coefficient and larger DWI signal intensities. Moreover, the simulation results indicated the dependences of important DWI parameters—b-value and Δ—on the percent signal changes after cell swelling. These results should be helpful for DW-fMRI experiments.

Acknowledgment

This work was supported by a Grant-in-Aid for JSPS Fellows (No. 023·5348).

References

[1] A. Darquié, J. Poline, C. Poupon, H. Saint-Jalmes, and D. Le Bihan, "Transient decrease in water diffusion observed in human occipital cortex during visual stimulation," Proc. National Academy of Sciences, vol.98, no.16, pp.9391–9395, 2001.
[2] D. Le Bihan, S. Urayama, T. Aso, T. Hanakawa, and H. Fukuyama, "Direct and fast detection of neuronal activation in the human brain with diffusion MRI," Proc. National Academy of Sciences, vol.103, no.21, pp.8263–8268, 2006.
[3] J. Kershaw, M. Tomiyasu, K. Kashikura, Y. Hirano, H. Nonaka, M. Hirano, H. Ikehira, I. Kanno, and T. Obata, "A multi-compartmental se-bold interpretation for stimulus-related signal changes in diffusion-weighted functional MRI," NMR in Biomedicine, vol.22, no.7, pp.770–778, 2009.
[4] T. Aso, S. Urayama, C. Poupon, N. Sawamoto, H. Fukuyama, and D. Bihan, "An intrinsic diffusion response function for analyzing diffusion functional MRI time series," NeuroImage, vol.47, no.4, pp.1487–1495, 2009.
[5] S. Kohno, N. Sawamoto, S. Urayama, T. Aso, K. Aso, A. Seiyama, H. Fukuyama, and D. Le Bihan, "Water-diffusion slowdown in the human visual cortex on visual stimulation precedes vascular responses," J. Cerebral Blood Flow & Metabolism, vol.29, no.6, pp.1197–1207, 2009.
[6] R. Andrew and B. MacVicar, "Imaging cell volume changes and neuronal excitation in the hippocampal slice," Neuroscience, vol.62, no.2, pp.371–383, 1994.
[7] T. Jin and S. Kim, "Functional changes of apparent diffusion coefficient during visual stimulation investigated by diffusion-weighted gradient-echo fMRI," NeuroImage, vol.41, no.3, pp.801–812, 2008.
[8] T. Truong and A. Song, "Cortical depth dependence and implications on the neuronal specificity of the functional apparent diffusion coefficient contrast," NeuroImage, vol.47, no.1, pp.65–68, 2009.
[9] A. Song and S. Gangstead, "The spatial and temporal characteristics of the apparent-diffusion-coefficient-dependent fMRI signal changes during visual stimulation," J. Neural Engineering, vol.1, p.32, 2004.
[10] S. Nagahara, T. Oida, and T. Kobayashi, "Dependence of diffusion weighted MR signal intensities on imaging parameters and restricted size," Transaction of the Japanese Society for Medical and Biological Engineering, vol.48, no.3, pp.281–290, 2010 (in Japanese).
[11] Y. Assaf, R. Freidlin, G. Rohde, and P. Basser, "New modeling and experimental framework to characterize hindered and restricted water diffusion in brain white matter," Magnetic Resonance in Medicine, vol.52, no.5, pp.965–978, 2004.
[12] T. Kobayashi, "New MRI technologies -diffusion MRI and its application to functional neuroimaging and analyses of white matter integrity," Systems, Control, and Information, vol.54, no.2, pp.58–65, 2011 (in Japanese).
[13] J. Nolte, The human brain: An introduction to its functional anatomy, Mosby, 2002.
[14] P. Vestergaard-Poulsen, B. Hansen, L. Østergaard, and R. Jakobsen, "Microstructural changes in ischemic cortical gray matter predicted by a model of diffusion-weighted MRI," J. Magnetic Resonance Imaging, vol.26, no.3, pp.529–540, 2007.
[15] K. Harkins, J. Galons, T. Secomb, and T. Trouard, "Assessment of the effects of cellular tissue properties on ADC measurements by numerical simulation of water diffusion," Magnetic Resonance in Medicine, vol.62, no.6, pp.1414–1422, 2009.
[16] J. Frahm, K. Merboldt, W. Hanicke, and A. Haase, "Stimulated echo imaging," J. Magnetic Resonance (1969), vol.64, no.1, pp.81–93, 1985.
[17] S. Heiland, O. Dietrich, and K. Sartor, "Diffusion-weighted imaging of the brain: Comparison of stimulated- and spin-echo echo-planar sequences," Neuroradiology, vol.43, no.6, pp.442–447, 2001.

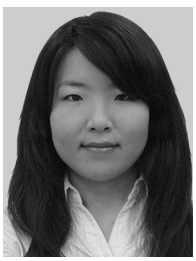

Shizue Nagahara received the B.E. and M.E. degrees from Kyoto University, Kyoto, Japan, in 2009 and 2011, respectively. From 2011, she is a doctral course student in the Department of Electrical Engineering, Graduate School of Engineering, Kyoto University. Her research interests include functional neuroimaging and magnetic resonance imaging. She is a member of Japanese Society for Magnetic Resonance in Medicine (JSMRM) and Japanese Society for Medial and Biological Engineering (JSMBE).

Takenori Oida received the B.E., M.E. and Ph.D. degrees in Systems Science, Graduate School of Informatics, Kyoto University, Kyoto, Japan, in 2001, 2003, and 2006, respectively. Since 2006, he has been an Assistant Professor in the Department of Electrical Engineering, Graduate School of Engineering, Kyoto University. His research interests include magnetic resonance imaging and medical image processing. He is a member of IEEE, International Society for Magnetic Resonance in Medicine (ISMRM), and Japanese Society for Medial and Biological Engineering (JSMBE).

Tetsuo Kobayashi received his B.S, M.S, and Ph.D. degrees from Hokkaido University, Sapporo, Japan in 1979, 1981 and 1984, respectively. From 2004, he is a professor of the department of electrical engineering, Kyoto University, Kyoto, Japan. His research interests include functional neuroimaging, cognitive neuroscience, optically-pumped atomic magnetometer and ultra-low field MRI. He is a councilor of Institute of Complex Medical Engineering and Japanese Society for Electromagnetic Topography (JSBET). He is also a member of IEEE and Organization for Human Brain Mapping (OHBM).